

1 **Performance evaluation of multiple satellite rainfall products for Dhidhessa River Basin**
2 **(DRB), Ethiopia**

3 **Gizachew Kabite Wedajo^{a,b*}, Misgana Kebede Muleta^c, Berhan Gessesse Awoke^{b,d}**

4 ^aDepartment of Earth Sciences, Wollega University, P.O.Box 395, Nekemte, Ethiopia

5 ^bDepartment of Remote Sensing, Entoto Observatory Research Center, Ethiopia Space Science
6 Technology Institute, P.O.Box 33679, Addis Ababa, Ethiopia

7 ^cDepartment of Civil and Environmental Engineering, California Polytechnic State University,
8 San Luis Obispo, California, 93407

9 ^dDepartment of Geography and Environmental Studies, Kotebe Metropolitan University, Addis
10 Ababa, Ethiopia

11 *Correspondence: Email: Kabiteg@gmail.com

12

13 **Abstract**

14 *Precipitation is crucial driver of hydrological processes. Ironically, a reliable characterization*
15 *of its spatiotemporal variability is challenging. Ground-based rainfall measurement using rain*
16 *gauges is more accurate. However, installing a dense gauging network to capture rainfall*
17 *variability can be impractical. Satellite-based rainfall estimates (SREs) could be good*
18 *alternatives, especially for data-scarce basins like in Ethiopia. However, SREs rainfall is*
19 *plagued with uncertainties arising from many sources. The objective of this study was to*
20 *evaluate the performance of the latest versions of several SREs products (i.e., CHIRPS2,*
21 *IMERG6, TAMSAT3 and 3B42/3) for the Dhidhessa River Basin (DRB). Both statistical and*
22 *hydrologic modelling approaches were used for the performance evaluation. The Soil and*
23 *Water Analysis Tool (SWAT) was used for hydrological simulations. The results showed that*
24 *whereas all four SREs products are promising to estimate and detect rainfall for the DRB, the*
25 *CHIRPS2 dataset performed the best at annual, seasonal and monthly timescales. The*
26 *hydrologic simulation based evaluation showed that SWAT's calibration results are sensitive*
27 *to the rainfall dataset. The hydrologic response of the basin is found to be dominated by the*
28 *subsurface processes, primarily by the groundwater flux. Overall, the study showed that both*
29 *CHIRPS2 and IMERG6 products could be reliable rainfall data sources for hydrologic*
30 *analysis of the DRB. Moreover, climatic season of the DRB influences rainfall and streamflow*
31 *estimation. Such information is important for rainfall estimation algorithm developers.*

32 **Keywords:** *Satellite-based rainfall estimates; Dhidhessa River Basin; Performance evaluation;*
33 *Statistical evaluation; Hydrological modelling performance.*

34

35 **1. Introduction**

36 Precipitation is an important hydrological component (Behrangi et al., 2011; Meng et
37 al., 2014). Accurate representation of its spatiotemporal variability is crucial to improves
38 hydrological modelling (Grusson et al., 2017). Ironically, precipitation is one of the most
39 challenging hydrometeorological data to be accurately represented (Yong et al., 2014).
40 Climatic and topographic conditions are the primary factors that affect the accuracy of rainfall
41 measurements.

42 Rainfall is measured either using ground-based (i.e., rain gauge and radar) or satellite
43 sensors, where all measurement methods exhibit limitations (Thiemig et al., 2013). In addition,
44 Commercial Microwave Links (CML) is introduced recently as cheap and fast rainfall
45 estimation method (Smiatek et al., 2017) but not fully tested methodology (Nebuloni et al.,
46 2020). Ground-based rainfall measurements using rain gauge is a direct and generally accurate
47 near the sensor location. However, rain gauges, for instant, either are of poor density to
48 represent spatial and temporal variability of precipitation, or may not even exist in many basins
49 especially in developing countries (Behrangi et al., 2011). Rain gauge based rainfall
50 measurement techniques provide point measurements and subject to missing data due to mainly
51 measurement errors (Kidd et al., 2012; Maggioni et al., 2016). It may also be infeasible to
52 install and maintain dense ground-based gauging stations in remote areas like mountains,
53 deserts, forests and large water bodies (Dinku et al., 2018; Tapiador et al., 2012). On the other
54 hand, radar-based rainfall measurement technique covers larger area and provides rainfall data
55 at high spatial and temporal scales (Sahlaoui and Mordane, 2019). However, radar rainfall
56 measurements have limitations due to attenuation of radar signal by several features that
57 negatively affect the quality of rainfall measurement (Villarini and Krajewski, 2010; Berne and
58 Krajewski, 2013; Sahlaoui and Mordane, 2019). Satellite-based rainfall estimates (SREs),
59 however, provide high-resolution precipitation data including in areas where ground-based
60 rainfall measurements are impractical, sparse, or non-existent (Stisen and Sandholt, 2010).

61 Consequently, high-resolution precipitation products have been developed over the last
62 three decades. These products include Tropical Rainfall Measuring Mission (TRMM) Multi-
63 satellite Precipitation Analysis (TMPA; Huffman et al., 2007), the Precipitation Estimation
64 from Remote Sensing Information Using Artificial Neuron Networks (PERSIANN;
65 Sorooshian et al., 2000), Climate Prediction Center (CPC) morphing algorithm (CMORPH)
66 (Joyce et al., 2004), African Rainfall Climatology (ARC) (Xie and Arkin 1995), Tropical

67 Applications of Meteorology using SATellite (TAMSAT) (Maidment et al., 2017) and the
68 Climate Hazards Group Infrared Precipitation with Stations (CHIRPS) (Funk et al., 2015).
69 The consistency, spatial coverage, accuracy and spatiotemporal resolution of SREs have been
70 improved over time (Behrangi et al., 2011).

71 As indirect rainfall estimation techniques, SREs products possess uncertainties
72 resulting from errors in measurement, sampling, retrieval algorithm, and bias correction
73 processes (Dinku et al., 2010; Gebremichael et al., 2014; Tong et al., 2014). Local topography
74 and climatic conditions can also affect the accuracy of SREs estimation (Bitew and
75 Gebremichael, 2011). Hence, SREs products should be carefully evaluated before using the
76 products for any application. Statistical and hydrological modelling are two common methods
77 for evaluating SREs. The statistical evaluation method examines the intrinsic precipitation data
78 quality including its spatiotemporal characteristics via pairwise comparison of the SREs
79 products and ground observations. Scale mismatches between area-averaged SRE data and
80 point-like ground-based measurements is the most critical drawback. The hydrological
81 modelling method evaluates the performance of a SREs product for a specific application such
82 as streamflow predictive ability at watershed scale (Su et al., 2017). The two methods
83 complement each other where the statistical method provides information on data quality while
84 the hydrological model technique assesses the usefulness of the data for hydrological
85 applications (Thiemig et al., 2013). However, most studies used only statistical evaluation
86 methods (e.g., Dinku et al., 2018; Ayehu et al., 2018).

87 Studies have recommended SREs products for data scarce basins (Behrangi et al., 2011;
88 Bitew and Gebremichael, 2011; Thiemig et al., 2013). However, there is no consensus
89 regarding “best” SREs product for different climatic regions. Nesbitt et al. (2008) found that
90 CMORPH and PERSIANN produced higher rainfall rates compared to TRMM for the
91 mountain ranges of Mexico. Dinku et al. (2008) reported better performance of the TRMM and
92 CMORPH products in Ethiopia and Zimbabwe whereas PERSIANN outperformed TRMM in
93 South America according to de Goncalves et al. (2006). Interestingly, the performance of SREs
94 products seems to differ even within a basin. For the Blue Nile basin in Ethiopia, for example,
95 CMORPH overestimated precipitation for the lowland areas but underestimated for the
96 highlands (Bitew and Gebremichael, 2011; Habib et al., 2012; Gebremichael et al., 2014). The
97 discrepancy in the findings of these studies shows the performance of SREs varies with region,
98 topography, season, and climatic conditions of the study area (Kidd and Huffman, 2011;

99 Seyyedi et al., 2015; Nguyen et al., 2018; Dinku et al., 2018). As such, many studies have
100 recommended SREs evaluation at a local scale to verify its performance for specific
101 applications (Hu et al., 2014; Toté et al., 2015; Kimani et al., 2017; Ayehu et al., 2018).

102 Studies have examined the performance of SREs in Ethiopia (Haile et al., 2013;
103 Worqlul et al., 2014; Ayehu et al., 2018; Dinku et al., 2018). However, majority of these studies
104 used the statistical method to evaluate SREs, and no study has been completed for the
105 Dhidhessa River Basin (DRB). With only 0.32 rain gauges per 1000 km², the DRB meets the
106 World Meteorological Organization (WMO) data-scarce basin classification (WMO, 1994).
107 Evaluating the performance of various SREs products in terms of characterizing the
108 spatiotemporal distribution of rainfall in the DRB could assist with the planning and
109 management of existing and planned water resources projects in the river basin.

110 SREs have been continuously updated to minimize bias and uncertainty. Evaluating
111 and validating improved products for various climatic regions would be valuable (Kimani et
112 al., 2017). Recently improved SREs products include Tropical Rainfall Measuring Mission
113 (TRMM) Multi-Satellite Precipitation Analysis version 7 (here after referred to as 3B43 for
114 monthly and 3B42 for daily products), Climate Hazards Group Infrared Precipitation with
115 Stations version 2 (CHIRPS2), Tropical Applications of Meteorology using SATellite version
116 3 (TAMSAT3) and Integrated Multi-satellitE Retrievals for GPM version 6B (IMERG6).
117 Studies have reported improvements of these new versions compared to their predecessors.
118 However, to the best of authors' knowledge, the rainfall detection and hydrological simulation
119 capability of these SREs datasets were not evaluated for the basins in Ethiopian including the
120 DRB. This study examined the latest SREs products in terms of their rainfall detection and
121 estimation skills, and improving hydrological prediction for DRB, a medium-sized river basin
122 with scarce gauging data. As such, the objectives of this study were: 1) to evaluate the intrinsic
123 rainfall data quality and detection skills of multiple SREs products (i.e., 3B42/3, CHIRPS2,
124 TAMSAT3, and IMERG6), and 2) to examine hydrologic prediction performances of SREs for
125 the DRB. The Soil and Water Assessment Tool (SWAT), a physically based semi-distributed
126 model that has performed well in humid tropical regions like Ethiopia, was used for the
127 hydrologic simulation.

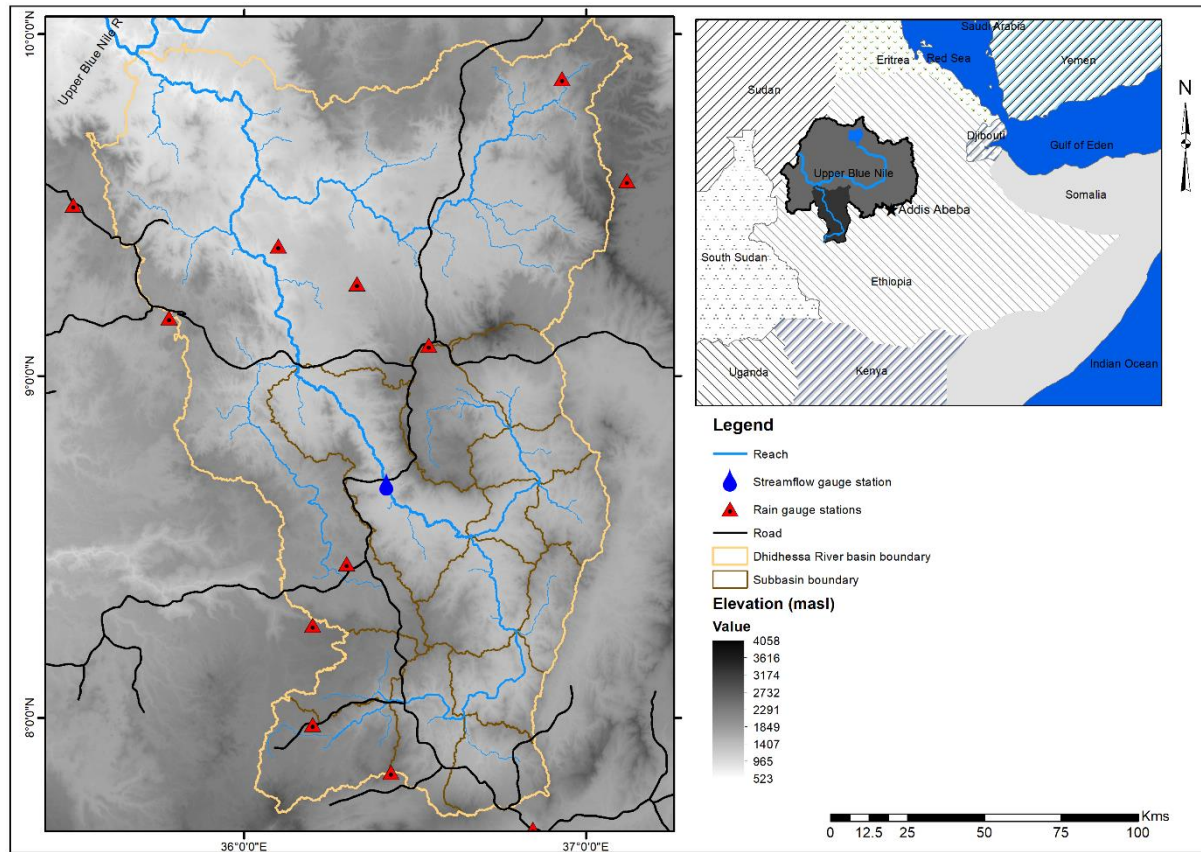
128

129 **2. Methods and Materials**

130 **2.1. Descriptions of the study area**

131 The Dhidhessa River drains to the Blue Nile River (Figure 1). It is one of the largest
132 and most important river basins in Ethiopia in terms of its physiography and hydrology
133 (Yohannes, 2008). Located between 7°42'43"N to 10°2'55"N latitude and 35°31'23"E to
134 37°7'60"E longitude, the river basin exhibits highly variable topography that ranges from 619
135 m to 3213 m above mean sea level (a.m.s.l). The Dhidhessa River starts from the Sigo
136 mountain ranges and travels 494 km before it joins the Blue Nile River around the Wanbara
137 and Yaso districts. The outlet considered for this study is the confluence of the Dhidhessa River
138 and the Blue Nile River which covers a total drainage area of 28,175 km². The River basin has
139 many perennial tributaries (Figure 1).

140 Temperature and precipitation in the Dhidhessa River basin exhibit substantial spatial
141 and seasonal variability. The mean maximum and minimum daily air temperatures in the river
142 basin range from 20-33°C and 6-19 °C, respectively. The long-term mean annual rainfall ranges
143 from 1200 mm to 2200 mm in the river basin. Soils in the DRB are generally deep and have
144 high organic content implying they have high infiltration potential. The dominant soil type is
145 Acrisols while Cambisols and Nitisols are common (OWWDSE, 2014). Igneous, sedimentary
146 and metamorphic rocks are common but igneous rock, particularly basalt, is dominant in the
147 basin (GSE, 2000). Forest, shrubland, grassland, and agriculture are the dominant land cover
148 types in the basin (Kabite et al., 2020). Major crops include perennial and cash crops like
149 coffee, Mango, and Avocado (OWWDSE, 2014).



150

151 Figure 1. Location map of Dhidhessa River basin with ground stations (USGS, 1998).

152 **2.2. Data sources and descriptions**

153 For this study, we used different spatial and temporal datasets such as Digital Elevation
 154 Model (DEM), climate, streamflow, soil and land cover from different sources (Table 1).

155 Table 1. Data description and sources.

Data type	Data periods	Resolution	Sources
SRTM DEM	1998	30 * 30 m	USGS
3B42/3	2001-2014	0.25° (~25 km)	NASA & JAXA
CHIRPS2	2001-2014	0.05° (~5 km)	USGS & Climate Hazard Group
TAMSAT3	2014-2014	0.0375° (~4 km)	Reading University
IMERG6	2001-2014	0.1° (~10 km)	NASA & JAXA
Streamflow data	2001-2014	Daily	EMoWI
Meteorological data	2001-2014	Daily	NMA
Land cover	2001	30*30 m	Kabite et al. (2020)
Soil map	2013/14	variable	EMoWI, FAO & OWWDSE

156 Shuttle Radar Thematic Mapper (SRTM) derived Digital Elevation Model (DEM) of
157 30*30 m spatial resolution was obtained from the United States Geological Survey (USGS). It
158 is one of the input data for SWAT model from which topographic and drainage parameters
159 (e.g., drainage pattern, slope and watershed boundary) were derived. Soil map was obtained
160 from source described in Table 1. Soil physical properties required for SWAT model were
161 derived from the soil map. Supervised image classification was used to prepare land cover map
162 of 2001. Together with land cover and soil maps, DEM was used to create Hydrologic Response
163 Units (HRUs).

164 Rainfall data for nine stations within the river basin and for three nearby stations (Figure
165 1), from 2001 to 2014 were obtained from the National Meteorological Agency (NMA) of
166 Ethiopia. The rainfall data was used to evaluate the SREs using the statistical and hydrological
167 modelling evaluation methods. In addition, Enhanced National Climate Time-series Service
168 (ENACTS) gridded (4 m *4 m) minimum and maximum air temperature data was obtained
169 from the National Meteorological Agency (NMA) of Ethiopia. Daily streamflow data from
170 2001 to 2014 was obtained for a station near the town of Arjo (Figure 1) from Ethiopian
171 Ministry of Water, Irrigation and Energy (EMoWI).

172 The hydrometeorological stations used for this study were selected due to their long-
173 term records and better data quality. The observed streamflow was used to calibrate and
174 validate SWAT model. Land use map for 2001 and soil map were obtained from Kabite et al.
175 (2020) and Ethiopian Ministry of Water, Irrigation and Energy (EMoWI), respectively.

176 **2.2.1. Satellite rainfall products**

177 The Satellite Rainfall Estimates (SREs) considered in this study include 3B42/3,
178 TAMSAT3, CHIRPS2 and IMERG6. These datasets were selected because of several reasons
179 including that they: i) have relatively high spatial resolution, ii) are gauge-adjusted products,
180 iii) are the latest products and have been found to perform well by recent studies, and iv) were
181 not compared for the basins in Ethiopia particularly IMERG6.

182 The TMPA provides rainfall products for area covering 50°N-50°S for the period of
183 1998 to present at 0.25°*0.25° and 3h spatial and temporal resolution, respectively. The 3h
184 rainfall product is aggregated to daily (3B42) and monthly (3B43) gauge-adjusted post real
185 time precipitation. The performance of the 3B42v7 is superior compared to its predecessor (i.e.,

186 3B42v6) and the real time TMPA product (3B42RT) (Yong et al., 2014). The 3B43 was used
187 in this study for the statistical evaluation while the 3B42 was used for the hydrological
188 performance evaluation. The detail description is given by Huffman et al. (2007).

189 TAMSAT3 algorithm estimates precipitation in an indirect method using cloud-index
190 method, which compares the cold cloud duration (CCD) with predetermined temperature
191 threshold. The CCD is the length of time that a satellite pixel is colder than a given temperature
192 threshold. The algorithm calibrates the CCD using parameters that vary seasonally and spatially
193 but constant from year to year. This makes interannual variations in rainfall to depend only on
194 the satellite observation. The dataset covers the whole Africa at ~4 km and 5-day (pentadal)
195 resolutions for the period of 1983 to present. The original 5-day temporal resolution is
196 disaggregated to daily time-step using daily CCD from which monthly data are derived.
197 TAMSAT3 algorithm are improved compared to its processor (i.e., TAMSAT2). The detail is
198 described in Maidment et al. (2017).

199 The Climate Hazards Group InfraRed Precipitation with Stations (CHIRPS) is a quasi-
200 global precipitation product with ~5km (0.05°) spatial resolution and is available at daily,
201 pentadal (5-day) and monthly timescales. The CHIRPS precipitation data is available from
202 1981 to present. It is gauge-adjusted dataset, which is calculated using weighted bias ratios
203 rather than using absolute station values, which minimizes the heterogeneity of the dataset
204 (Dinku et al., 2018). The latest version of CHIRPS that uses more station data (i.e., CHIRPS
205 version 2 here after CHIRPS2) was used in this study. Detail description of CHIRPS2 is given
206 in Funk et al. (2015).

207 The Global Precipitation Measurement (GPM) is the successor of TRMM with better
208 rainfall detection capability. GPM provides precipitation measurements at 0.1° and half-hourly
209 spatial and temporal resolution. Integrated Multi-satellitE Retrievals for GPM (IMERG) is one
210 of the GPM precipitation product estimated from all constellation microwave sensors, IR-based
211 observations from geosynchronous satellites, and monthly gauge precipitation data. IMERG is
212 the successor algorithm of TMPA. The IMERG products includes Early Run (near real-time
213 with a latency of 6h), Late Run (reprocessed near real-time with a latency of 18 h) and Final
214 Run (gauge-adjusted with a latency of four months). The IMERG Final Run product provides
215 more accurate precipitation information compared to the near-real time products as it is gauge-
216 adjusted. The latest release of GPM IMERG Final Run version 6B (IMERG6) was used for
217 this study. The detail is given by Huffman et al. (2014).

218 In this study, the performances of 3B42/3, TAMSAT3, CHIRPS2 and IMERG6 rainfall
219 products were evaluated statistically and hydrologically. All the SREs considered in this study
220 are gauge-corrected, and thus bias correction may not be required. Thus, rain gauge stations
221 (e.g., Jimma and Nekemte) that were used for calibrating the SREs datasets were excluded for
222 fair comparison. The lists of rain gauge stations used for this study are shown in Figure 1 and
223 Appendix Table 1. The detail summaries of the data types used for this study are shown in
224 Table 1.

225 **2.3. Methodology**

226 Satellite rainfall estimates offer several advantages compared to the conventional
227 methods but can also be prone to multiple errors. Rainfall detection capability of SREs can be
228 affected by local climate and topography (Xue et al., 2013; Meng et al., 2014). Therefore,
229 performance of SREs should be examined for a particular area before using the products for
230 any application (Hu et al., 2014; Toté et al., 2015; Kimani et al., 2017).

231 The two common SREs performance evaluation methods are statistical (i.e., ground-
232 truthing) and hydrological modelling performance (Behrangi et al., 2011; Bitew and
233 Gebremichael, 2011; Thiemig et al., 2013, Abera et al., 2016; Jiang et al., 2017), and were used
234 in this study. The methods complement each other and their combined application is
235 recommended for more reliable SREs evaluation techniques. The statistical evaluation method
236 involves pairwise comparison of SREs and the rain gauge products. The method provides
237 insight into the intrinsic data quality whereas the modelling approach assesses the usefulness
238 of the data for a desired application (Thiemig et al., 2013). Statistical evaluation was performed
239 for all the SREs products considered in this study (i.e., 3B43, CHIRPS2, TAMSAT3 and
240 IMERG6) to examine their rainfall detection skills. Continuous and categorical validation
241 indices were used to evaluate performance of the products. In addition, the SREs product and
242 gauge datasets were independently used as forcing to calibrate and verify SWAT model.
243 Accordingly, streamflow prediction performance of the rainfall products was evaluated
244 graphically and using statistical indices.

245 **2.3.1. Statistical evaluation of satellite rainfall estimates**

246 Statistical SREs evaluation method was conducted at monthly, seasonal and annual
247 timescales for the overlapping period of all the rainfall data sources (i.e., 2001-2014). A daily

248 comparison was excluded from this study due to weak performance reported in previous studies
249 (Ayehu et al., 2018; Zhao et al., 2017; Li et al., 2018). This is attributed to the measurement
250 time mismatch between ground and satellite rainfall products.

251 Two approaches are commonly used for the statistical evaluation method. The first
252 approach is pixel-to-pixel pairwise comparisons of the spatially interpolated gauge-based and
253 satellite-based data. The second approach is point-to-pixel pairwise comparison where satellite
254 rainfall estimates are extracted for each gauge locations and the satellite-gauge data pairs are
255 generated and compared. The second approach was used for this study. This is because the 12
256 rainfall stations considered in this study are unevenly distributed throughout the basin to
257 accurately represent spatial variability of rainfall in the DRB as required for the first approach.
258 As a result, we chose to extract gauge-satellite rainfall pair values at each rain gauge location
259 instead of interpolating the gauge measurements into gridded products.

260 Accordingly, 168 and 2016 paired data points were extracted for annual and monthly
261 analysis, respectively, and were evaluated using continuous validation indices such as Pearson
262 correlation coefficient (r), bias ratio ($BIAS$), Nash-Sutcliffe efficiency (E) and Root Mean
263 Square Error ($RMSE$). The Pearson correlation coefficient (r) evaluates how well the estimates
264 correspond to the observed values; $BIAS$ reflects how the satellite rainfall estimate over- or
265 under-estimate the rain gauge observations; E shows how well the estimate predicted the
266 observed time series. On the other hand, $RMSE$ measures the average magnitude of the estimate
267 errors. The summary of performance indices are presented in Table 2.

268

269 Table 2. SREs evaluation indices, mathematical descriptions and perfect score.

Indices	Mathematical expression	Description	Perfect score
Pearson correlation	$r = \frac{\sum(R_g - \bar{R}_g)(R_s - \bar{R}_s)}{\sqrt{\sum(R_g - \bar{R}_g)^2} \sqrt{\sum(R_s - \bar{R}_s)^2}}$	R_g is gauge rainfall observation; R_s satellite rainfall estimates; \bar{R}_g is average gauge rainfall observation; \bar{R}_s is average satellite rainfall estimates. The value ranges from -1 to 1.	1
Root mean square error (mm)	$RMSE = \sqrt{\frac{\sum(R_g - R_s)^2}{n}}$	n is the number of data pairs; the value ranges from 0 to ∞	0
Bias ratio (BIAS)	$BIAS = \frac{\sum R_s}{\sum R_g}$	A value above (below) 1 indicates an aggregate satellite overestimation (underestimation) of the ground precipitation amounts.	1
Relative bias (RB)	$RB = \frac{\sum(R_s - R_g)}{\sum R_g} * 100$	Describes the systematic bias of the SREs; positive values indicate overestimation while negative values indicate underestimation of precipitation amounts.	0
Mean Error (ME)	$ME = \frac{1}{n} \sum_{i=1}^n (R_s - R_g)$	Describes the average errors of the SREs relative to the observed rainfall data.	0
Nash-Sutcliffe of efficiency coefficient (E)	$E = 1 - \frac{\sum(R_s - R_g)^2}{\sum(R_g - \bar{R}_g)^2}$	The value ranges from $-\infty$ to 1; $0 < E \leq 1$ acceptable while $E \leq 0$ is unacceptable	1
Percent bias (%)	$PBIAS = \frac{\sum(Q_o - Q_s)}{\sum(Q_o)} * 100$	Q_o is observed discharge; Q_s is simulated discharge for the available pairs of data where $< \pm 15\%$ is very good	0
Coefficient of determination (r^2)	$r^2 = \left(\frac{\sum_{i=1}^n (O_i - \bar{O})(S_i - \bar{S})}{\sqrt{\sum_{i=1}^n (O_i - \bar{O})^2} \sqrt{\sum_{i=1}^n (S_i - \bar{S})^2}} \right)^2$	O_i & \bar{O} is observed & average streamflow, respectively; S_i & \bar{S} is simulated and average, respectively. The value ranges from 0 to 1.	1
Nash-Sutcliffe coefficient of efficiency	$NSE = \frac{\sum(Q_o - \bar{Q}_o)^2 - \sum(Q_o - Q_s)^2}{\sum(Q_o - \bar{Q}_o)^2}$	\bar{Q}_o is mean value of the observed discharge for the entire time under consideration	1

270 In addition to the continuous validation indices, tercile categories (i.e., percentile-based
 271 evaluation) along with probability of exceedance were performed to test the performance of
 272 SREs in detecting low-and high-end values. The tercile (percentile) and probability of
 273 exceedance methods better evaluates rainfall detection capabilities of SREs for monthly time
 274 scale compared to the other categorical indices such as probability of detection (*POD*), false
 275 alarm ratio (*FAR*) and critical success index (*CSI*). This is because the *POD*, *FAR* and *CSI* are
 276 not effective for monthly-based analysis but effective for daily-based analysis.

277 Tercile is a set of data that are partitioned in to three equal groups each containing one-
278 third of the total data. To calculate terciles, percentiles were used for this study. Accordingly,
279 the low, middle and high terciles were defined using the 33th, 67th and 100th percentiles. As
280 such, the first 33 percentile is named as lower tercile (P33), the second 33 percentile is names
281 as medium tercile (P67) and the third 33 percentile is named as higher tercile (P100). On the
282 other hand, probability of exceedance was calculated as a percentage of a given events to be
283 equated or exceeded.

$$284 \quad P = \frac{m}{n+1} * 100 \quad (1)$$

285 where P represents the percentage probability that a given event will be equaled or exceeded
286 m represent ranks of the event value, with 1 being the largest possible value.
287 n total number of events or data points on records.

288 In general, SREs with $r > 0.7$ and relative bias (*RB*) within 10% can be considered as
289 reliable precipitation measurement sources (Brown, 2006; Condom et al., 2011). However,
290 attention should be given to certain indices depending on the application of the product (Toté
291 et al., 2015). For flood forecasting purpose, for example, underestimation of rainfall should be
292 avoided (i.e., mean error (*ME*) > 0 is desirable). In contrast, for drought monitoring,
293 overestimation must be avoided (i.e., *ME* < 0 is preferred) (Dembélé and Zwart, 2016).

294 **2.3.2. SWAT model setup**

295 Soil and Water Assessment Tool (SWAT) is a semi-distributed, deterministic and
296 continuous simulation watershed model that simulates many water quality and quantity fluxes
297 (Arnold et al., 2012). It is a physically based and computationally efficient model that has been
298 widely used for various hydrological and/or environmental application in different regions of
299 the world (Gassman et al., 2014). Furthermore, the capability of SWAT model to be easily
300 linked with calibration, sensitivity analysis and uncertainty analysis tools (e.g., SWAT-CUP)
301 made it more preferable.

302 SWAT model follows a two-level discretization scheme: i) sub-basin creation based on
303 topographic data and ii) Hydrological Response Unit (HRU) creation by further discretizing
304 the sub-basin based on land use and soil type. HRU is a basic computational unit assumed to
305 be homogeneous in hydrologic response. Hydrological processes are first simulated at the HRU
306 level and then routed at the sub-basin level (Neitsch et al., 2009). The SWAT model estimates

307 surface runoff using the modified United States Department of Agriculture (USDA) Soil
308 Conservation Service (SCS) curve number method. In this study, a minimum threshold area of
309 400 km² were used for determining the number of sub-basins and 5% threshold for the soil,
310 slope, and land use were used for the HRU definition. Accordingly, 13 sub basins and 350
311 HRUs are created for the Arjo gauging station as outlet.

312 **2.3.3. SWAT model calibration and validation**

313 Hydrologic modelling performance evaluation technique is commonly performed by
314 either calibrating the hydrologic model with gauge rainfall data and then validating with SREs,
315 (i.e., static parameters) or calibrating and validating the model independently with each rainfall
316 products (i.e., dynamic parameters) and then compare accuracies of the streamflow predicted
317 using the capacity of the rainfall products. The latter is preferred for watersheds such as the
318 DRB where gauging stations are sparse and unevenly distributed. Moreover, studies have
319 reported that independently calibrating the hydrologic model with SREs and gauge data
320 improves performance of the hydrological model (Zeweldi et al., 2011; Vernimmen et al.,
321 2012; Lakew et al., 2017).

322 Calibration, validation and sensitivity analysis of SWAT was done using the SWAT-
323 CUP software. The Sequential uncertainty fitting (SUFI-2) implemented in SWAT-CUP was
324 used in this study (Abbaspour et al., 2007). SUFI-2 provides more reasonable and balanced
325 predictions than the generalized likelihood uncertainty estimation (GLUE) and the parameter
326 solution (ParaSol) methods (Zhou et al., 2014; Wu and Chen et al., 2019) offered by the tool.
327 It also estimates parameter uncertainty attributed to input data, and model parameter and
328 structure as total uncertainty (Abbaspour, 2015). The total uncertainty in the model prediction
329 is commonly measured by *P*-factor and *R*-factor. *P*-factor represents the percentage of observed
330 data enveloped by the 95 percent prediction uncertainty (95PPU) simulated by the model. The
331 *R*-factor represents the ratio of the average width of the 95PPU band to the standard deviation
332 of observed data. For realistic model prediction, *P*-factor ≥ 0.7 and *R*-factor ≤ 1.5 is desirable
333 (Abbaspour et al., 2007, Arnold et al., 2012).

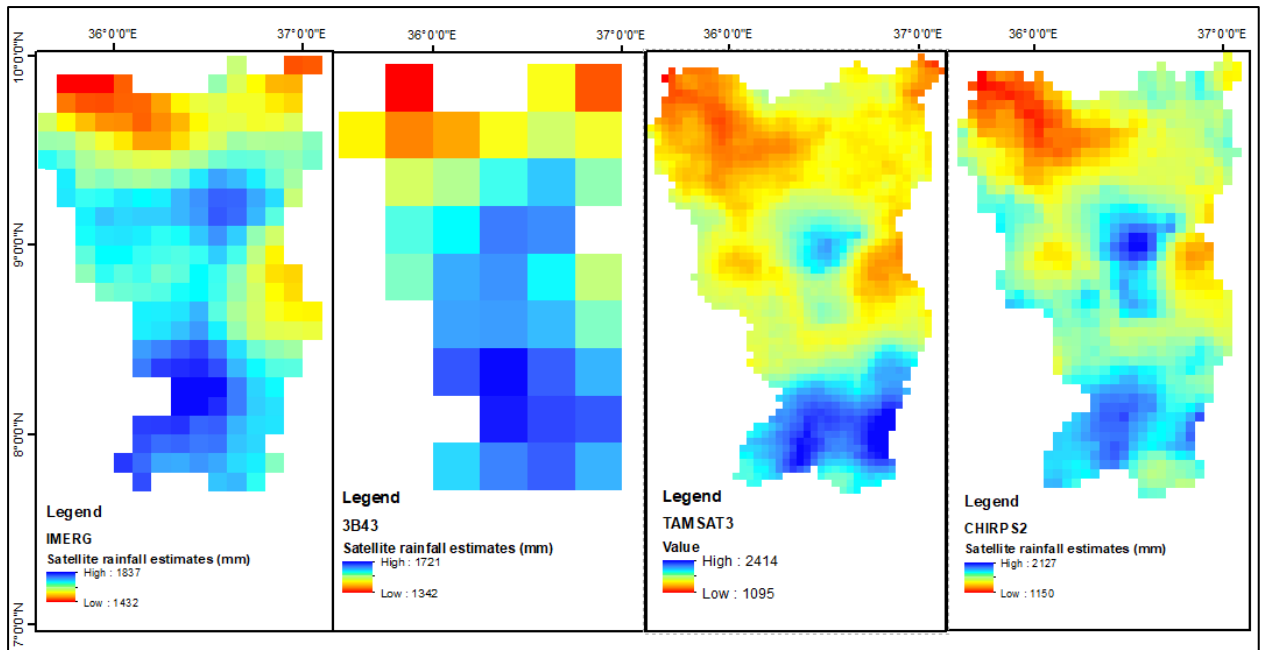
334 The first steps in SWAT model calibration and validation process is determining the
335 most sensitive parameters for a given watershed. For this study, 19 parameters were identified
336 based on the recommendations of previous studies (Roth et al., 2018; Lemann et al., 2019).
337 Global sensitivity analysis was performed on the 19 parameters from which 11 parameters were

338 found sensitive for the DRB, and were used for calibration, verification, and uncertainty
339 analysis. The hydrologic simulations were performed for the 2001 to 2014 period. Two years
340 of spin-up (warm-up) period (i.e., 2001 and 2002), and 6 years of calibration period (2003 to
341 2008), and 6 years of verification periods (2009 to 2014) were used. Graphical and statistical
342 measures were used to evaluate prediction capability of the rainfall datasets. Accordingly, the
343 performance of model forced by each rainfall datasets was tested using the most widely used
344 statistical indices (i.e., R^2 , NSE and $PBIAS$), in addition to the P -factor and R -factor.

345 **3. Results**

346 **3.1. Statistical evaluation**

347 Figure 2 compares mean annual spatial rainfall distributions of the DRB. Average
348 annual rainfall of the study area for the 2001 to 2014 period was 1682.09 mm/year (1150 to
349 2127 mm/year), 1698.59 mm/year (1432 to 1837 mm/year), 1699.06 mm/year (1092 to 2414
350 mm/year) and 1680.28 mm/year (1342 to 1721 mm/year) according to the CHIRPS2, IMERG6,
351 TAMSAT3 and 3B43 products, respectively. For reference, mean annual rainfall for the DRB
352 is 1650 mm/year based on the rain gauge data, which is within 1.8% to 3% of the estimates
353 provided by the products. However, total annual rainfall range estimates were substantially
354 different among the products. The decreasing rainfall trend from the southern (highlands) to
355 the northern (lowlands) part of the basin were captured by all products. In particular,
356 TAMSAT3 and CHIRPS2 captured the rainfall variability in better detail, perhaps due to their
357 high spatial resolution. On the other hand, resolution of the 3B43 rainfall product seems too
358 coarse to satisfactorily represent spatial variability of rainfall in the basin.

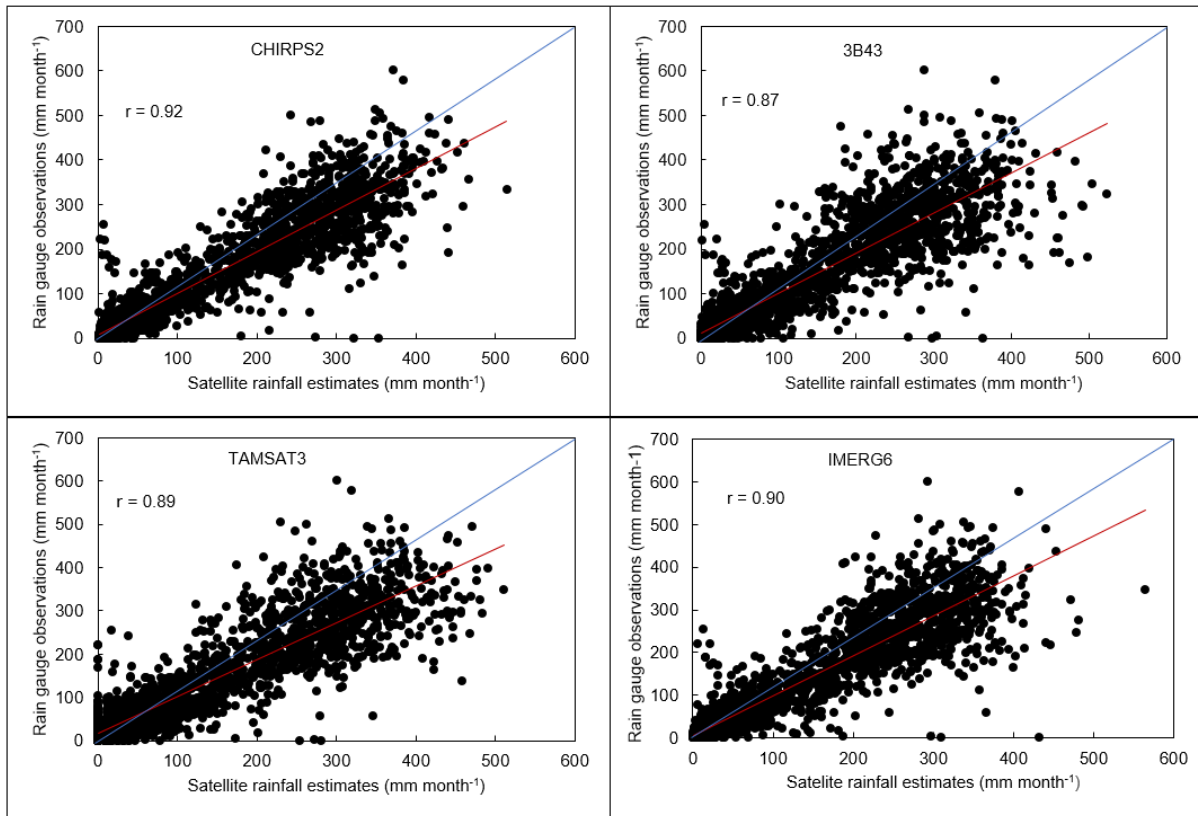


359
360 Figure 2. Spatial mean annual rainfall distribution of the four SREs for DRB (2001 to 2014)

361 Figures 3 to 5 show results of statistical evaluation indices calculated from rainfall from
 362 the rain gauges and from the SREs products. More specifically, Figures 3 and 4 show
 363 correlation coefficients for the annual and monthly timescales, respectively. The results show
 364 that all four SREs products produced rainfall that correlate better to the ground based rainfall
 365 observations at monthly timescale than at annual time scales. This is because performance of
 366 SREs improved with increased time aggregation and peaks at monthly timescale. More likely,
 367 the seasonal variability is much larger than the interannual variability. The seasonal variability
 368 is, apparently, captured reasonably well, causing a higher degree of correlation for monthly
 369 data. The values of statistical evaluation indices for all products are summarized in Table 3.
 370 The results show that the CHIRPS2 performed better for the DRB with relatively higher r and
 371 E , and lower $BIAS$, ME and $RMSE$ for annual and monthly timescales, respectively.

372 Table 3. Statistical evaluation indices of all SREs.

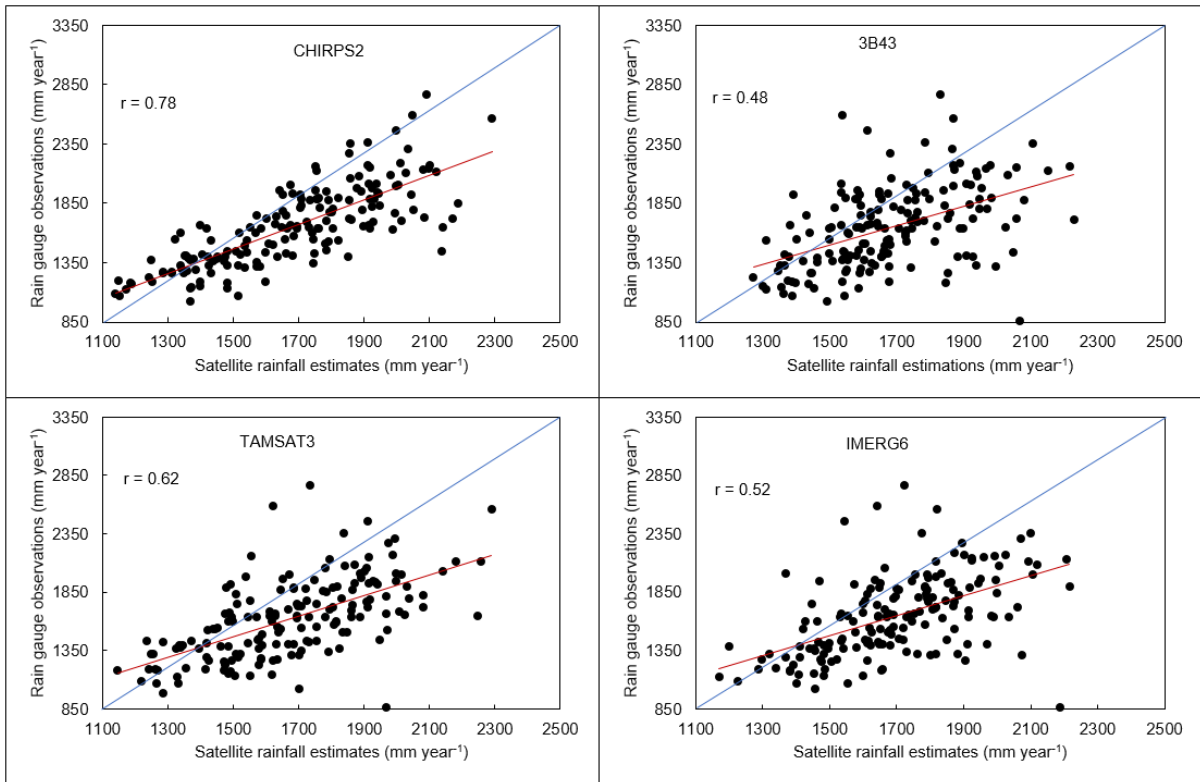
SREs	R		$BIAS$		ME		$RMSE$ (mm)		E	
	Annual	Monthly	Annual	Monthly	Annual	Monthly	Annual	Monthly	Annual	Monthly
CHIRPS2	0.78	0.92	1.01	1.01	25.94	2.70	214.36	50.48	0.51	0.84
3B43	0.48	0.87	1.02	1.02	30.58	2.55	306.34	62.05	0.76	0.76
IMERG6	0.52	0.90	1.03	1.03	48.87	4.07	299.55	56.95	0.39	0.80
TAMSAT3	0.62	0.89	1.03	1.03	51.46	2.67	274.00	61.28	0.77	0.77



373

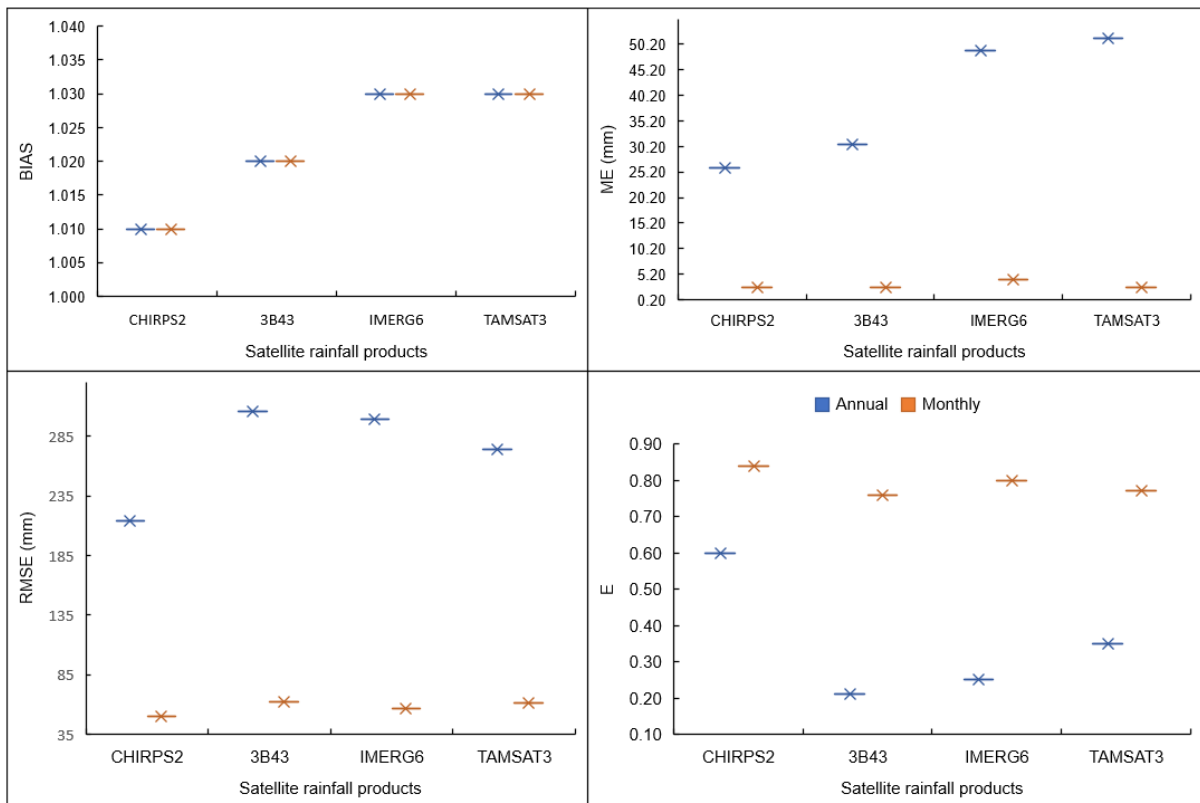
374 Figure 3. Correlation coefficient of the four SREs at monthly timescale over DRB.

375 Figures 3 to 5 and Table 3 show that generally, CHIRPS2 performed better than the
 376 other three products for the DRB. Correlation coefficients for both monthly and annual
 377 timescales as well as all the indices presented in Figure 5 favor CHIRPS2 indicating its superior
 378 performance. Relative performance of the other three SREs is inconsistent as it varies with the
 379 statistical indices used in this study. The 3B43 product, for example, performed worse based
 380 on Figure 3 and 4 (i.e., correlation coefficients for annual and monthly timescales) and *RMSE*
 381 and *E* (Figure 5), but performed better than the other two SREs based on *BIAS* and *ME*.



382

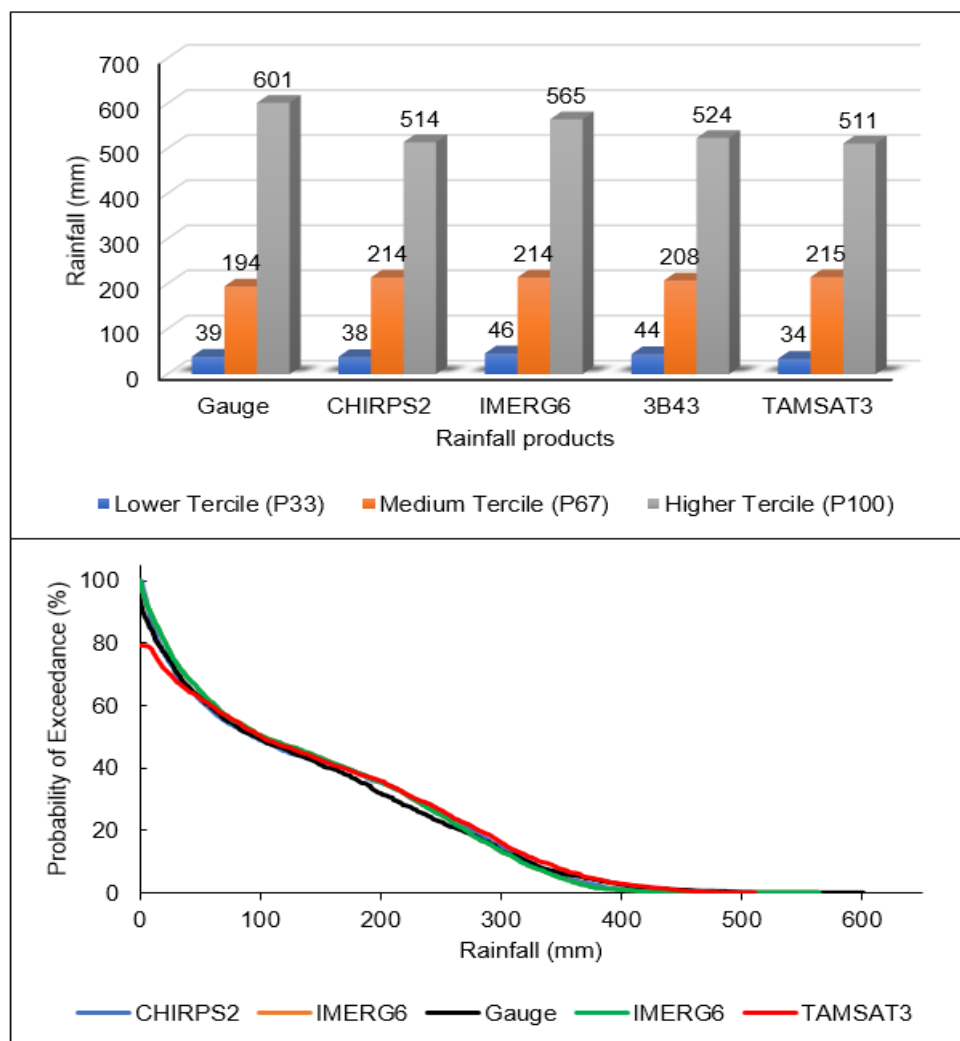
383 Figure 4. Annual correlation coefficient of the four SREs for the DRB.



384

385 Figure 5. Statistical indices of the four SREs for DRB at annual and monthly time scales.

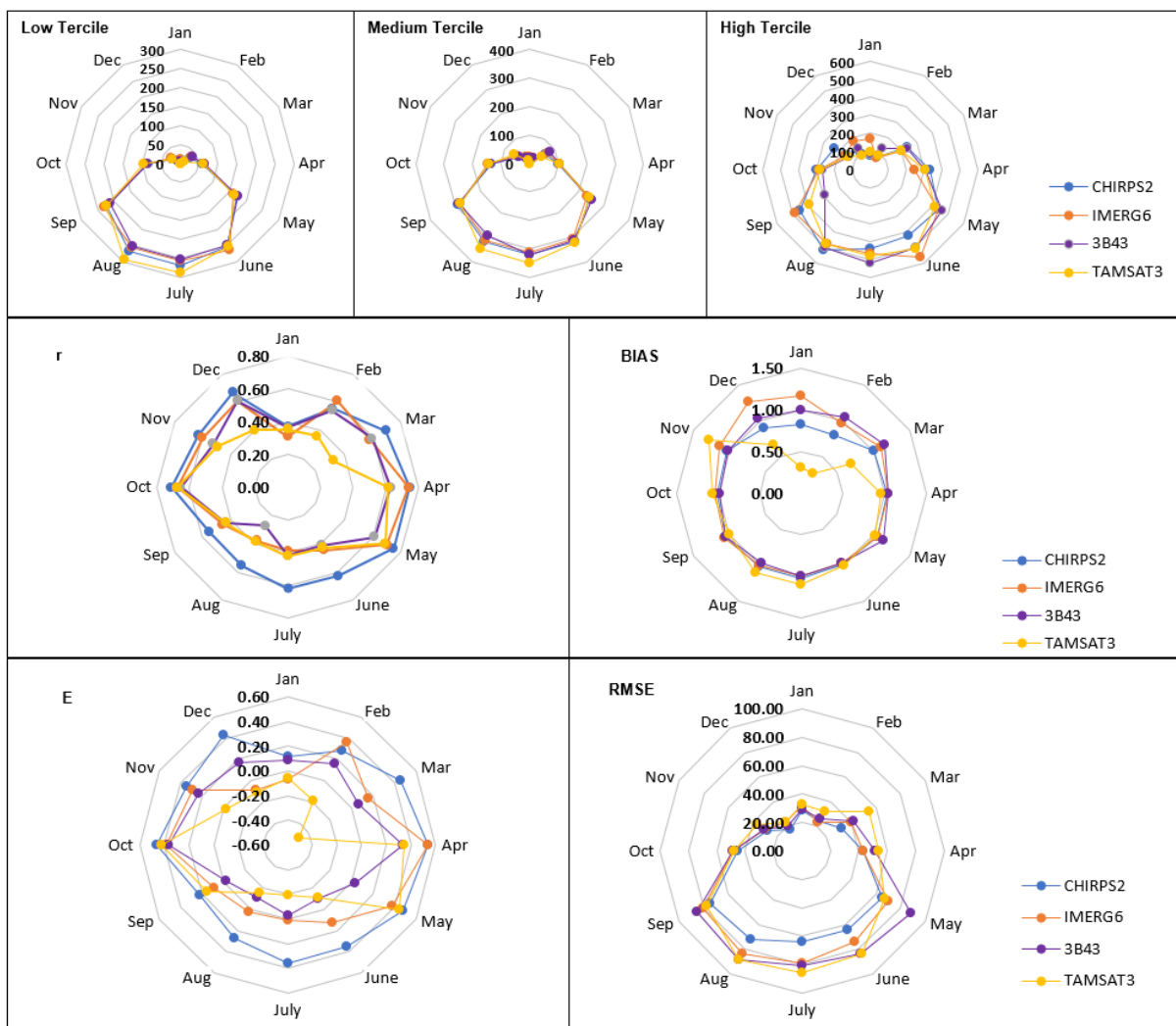
386 Tercile (percentile) categorical and probability of exceedance analysis result (Figure 6)
 387 show that all the SREs considered in this study have high rainfall detection capability for the
 388 DRB. Rainfall threshold used for this figure is 1mm/day. The lower tercile (33th *percentile*;
 389 P33), middle tercile (67th *percentile*;P67) and higher tercile (100th *percentile*;P100) of all
 390 SREs closer values with the corresponding gauge values indicating that the SREs detects
 391 rainfall for the DRB. However, CHIRPS2, 3B43 and IMERG6 have lower tercile, medium
 392 tercile and higher tercile much closer to the gauges, respectively. Moreover, the probability of
 393 exceedance further confirms the rainfall detection capability of the SREs considered in this
 394 study for the DRB. The probability of exceedance result indicated that TAMSAT3 has an 80%
 395 probability to exceed 0 mm, whereas the other products have near 100% probability. This is
 396 because TAMSAT3 has more observations with zero rainfall values compared to the other
 397 products. Overall, TAMSAT3 exhibited relatively less rainfall detection skill, which could be
 398 attributed to the relatively more sensitivity of TAMSAT3 to topographic effects.



399
 400

Figure 6. Tercile categories (top) and probability of exceedance of SREs.

401 Figure 7 shows seasonal SREs performance evaluation results. The figure generally
 402 shows that performance of the SREs varied from season to season and among the rainfall
 403 products. Main rainy season in the DRB is from June to September while short rainy season
 404 ranges from March to May but the rest is dry season (Figure 9). For example, CHIRPS2 is
 405 superior in detecting and estimating rainfall events for the DRB for all months (seasons). The
 406 rainfall detection and estimating capability of CHIRPS2 is better for rainy season compared to
 407 the dry season. Likewise, the rainfall detection capability of TAMSAT3 is stronger for the
 408 rainy season (May to November) but weaker for the dry season (December to April). Compared
 409 to the other SREs products, TAMSAT3 generally poorly correlated for all months (seasons),
 410 and its *BIAS* was the highest for rainy season but the lowest for the dry season.



411
 412 Figure 7. Seasonal statistical evaluation result comparison of each SREs for the DRB.

413

414 3.2. Hydrological modelling performance evaluation

415 The centroid of each sub basins were used as gauging locations, and used for extracting
416 rainfall for all the SREs rainfall datasets. Thus, each sub basins are represented by a separate
417 and dense gauges unlike that of the measured rainfall representation. The performance of the
418 rainfall products were evaluated using SWAT-CUP at monthly time steps.

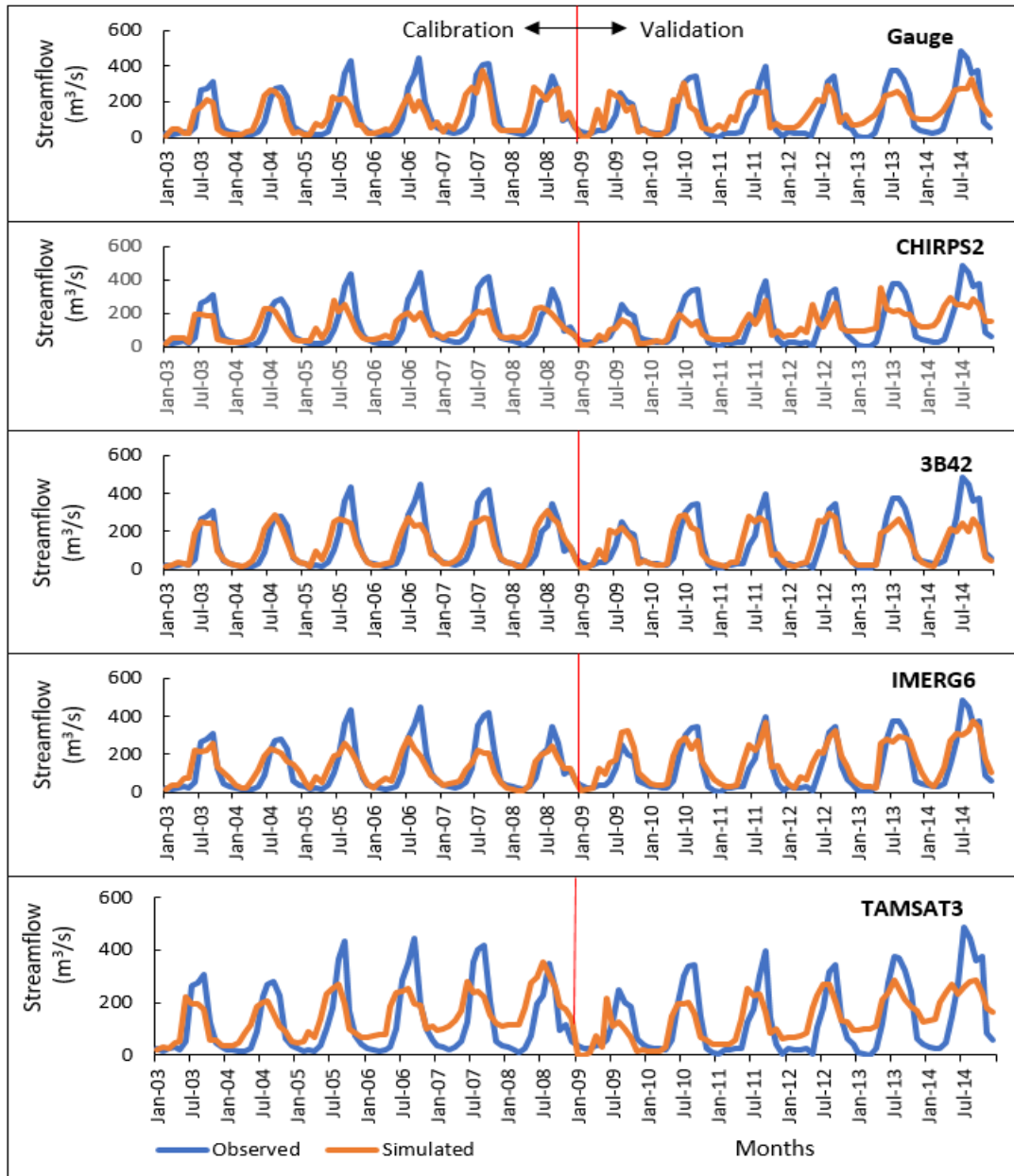
419 Table 4 shows details of the calibrated parameters including their ranges, best fit values,
420 sensitivity ranks when different rainfall datasets are used as inputs for the DRB. The best fit
421 values were multiplied by (1+ given value) and replaced by the given value for the parameters
422 with *r*-prefix and *v*-prefix, respectively. The table shows that ranges and the best fit values vary
423 from rainfall data source to another. This indicates the sensitivity of hydrological model
424 performance to rainfall products and thus accurate characterization of rainfall variability is very
425 critical for reliable hydrological predictions. This finding is consistent with studies that
426 reported that different precipitation datasets influence model performance, parameter
427 estimation and uncertainty in streamflow predictions (Sirisena et al., 2018; Goshime et al.,
428 2019). Relative sensitivity of the parameters also varied between the rainfall datasets. In
429 general, threshold depth of water in the shallow aquifer required for return flow to occur (mm)
430 (*GWQMN.gw*), base flow alpha factor (*ALPHA_BF.gw*), Groundwater delay (day)
431 (*GW_DELAY.gw*), deep aquifer percolation fraction (*RCHRG_DP.gw*), and runoff curve
432 number for moisture condition II (*CN2.mgt*) are top five sensitive parameters. This seems
433 indicate that groundwater processes dominate streamflow in the DRB. This could be attributed
434 to the dominantly deep and permeable soil, vegetated land surface and dominant tertiary
435 basaltic rocks in the DRB (Conway, 2000; Kabite and Gessesse, 2018). The groundwater
436 parameters can have a strong effect on the amount of streamflow that can cause over or
437 underestimation of streamflow. For this reason, the validation of streamflow was sorely
438 dependent on the rainfall products.

439

440 Table 4. Initial parameter ranges, fit values, and sensitivity ranks for rainfall data sources.

Parameters	Initial values	Gauge		CHIRPS2		IMERG6		3B42		TAMSAT3	
		Fit value	Rank	Fit value	Rank	Fit value	Rank	Fit value	Rank	Fit value	Rank
v_GWQMN.gw	0 to 5000	4936.02	1	201.64	3	3379.76	3	4784.74	1	-0.15	1
v_ALPHA_BF.gw	0 to 1	0.00	2	0.45	4	0.04	4	0.00	2	0.00	2
v_GW_DELAY.gw	0 to 500	339.10	3	29.02	5	34.76	6	391.13	4	318.08	3
v_RCHRG_DP.gw	0 to 1	0.02	4	0.44	7	0.04	5	0.30	3	0.04	4
r_CN2.mgt	-0.25 to 0	310.12	5	-0.25	11	-0.17	10	-0.13	5	-0.15	5
r_SOL_K.sol	0 to 2000	260.96	6	1086.63	9	391.90	11	286.12	6	447.41	6
v_CH_N2.rte	-0.01 to 0.3	0.74	7	0.02	1	0.05	1	0.29	8	0.61	7
v-CH_K2.rte	-0.01 to 500	310.12	8	354.51	2	426.08	2	256.15	7	298.36	8
v_GW_REVAP.gw	0.02 to 0.2	0.40	9	0.15	8	0.20	8	0.26	9	0.33	10
r_SOL_AWC.sol	-0.5 to 0.5	-0.01	10	-0.49	6	-0.19	7	-0.85	10	-0.59	9
v_REVAPMN.gw	0 to 500	170.26	11	14.52	10	381.84	9	142.11	11	176.48	11

441 Figure 8 compares the observed and the predicted streamflows for the calibration (2003
442 to 2008) and verification (2009 to 2014) periods for all five rainfall datasets. Goodness of the
443 streamflow predictions is also summarized in Table 5. The results show that the peak
444 streamflow is underestimated for all rainfall products, including gauges, but the streamflow
445 volume is generally overestimated. This could be due to the uncertainty of SREs for the
446 extreme rainfall events at daily scale (Jiang et al., 2017) and SWAT model error. The
447 overestimated streamflows could also be attributed to overestimation of rainfalls by the SREs
448 as described in the previous sections. Generally, the indices provided in Table 4 indicate that
449 the streamflow predictions are good for CHIRPS2, IMERG6, and satisfactory for the gauged
450 rainfall but not for TAMSAT3 and 3B42 according to Moriasi et al. (2017) classification
451 system. The performance of the SREs are consistent with the climatology of the products. Mean
452 monthly rainfall from 2001 to 2014 showed that TAMSAT3 and 3B42 deviate more from
453 observed rainfall while CHIRPS2 and IMERG6 are relatively closer (Figure 9).

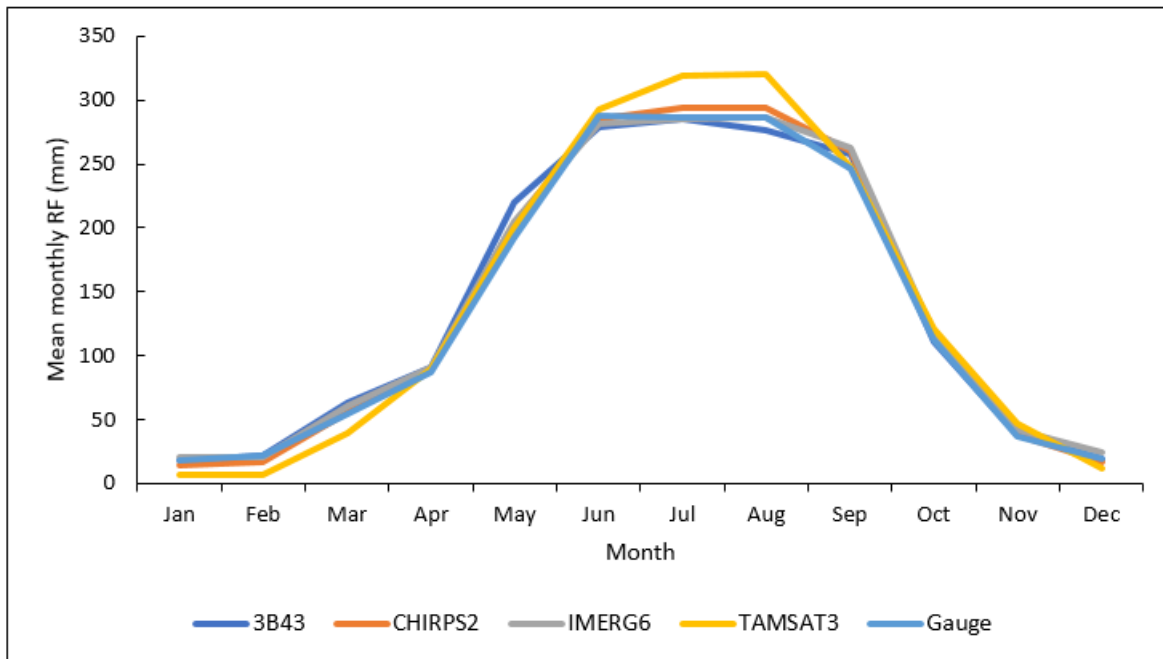


454

455 Figure 8. Graphical calibration and validation of streamflow at monthly scale.

456 Table 5. Calibration and validation results for the different rainfall products.

Rainfall products	Calibration					Validation				
	<i>NSE</i>	<i>R</i> ²	<i>PBIAS</i>	<i>P</i> -factor	<i>R</i> -factor	<i>NSE</i>	<i>R</i> ²	<i>PBIAS</i>	<i>P</i> -factor	<i>R</i> -factor
Gauge	0.55	0.54	2.8	0.43	0.55	0.54	0.57	-9.3	0.15	0.27
CHIRPS2	0.69	0.7	-2.5	0.72	0.64	0.65	0.66	5.3	0.46	0.58
IMERG6	0.65	0.67	2.2	0.70	0.66	0.73	0.78	-14.5	0.64	0.86
TAMSAT3	0.43	0.46	-16.7	0.31	2.94	0.48	0.48	-4.9	0.46	2.68
3B42	0.48	0.51	8.6	0.65	3.88	0.45	0.46	1.3	0.82	2.96



457
458 Figure 9. Mean monthly rainfall (2001 to 2014).

459 4. Discussion

460 The statistical SREs evaluation result showed that all the rainfall products captured the
 461 spatiotemporal rainfall variability of the DRB except the 3B43. Poor performance of 3B43 in
 462 capturing basin's rainfall variability is in agreement with findings of two previous studies done
 463 for other basins in Ethiopia (Dinku et al., 2008; Worqlul et al., 2014). The reasons could be
 464 attributed to the fact that gauge adjustment for 3B43 product did not use adequate gauge data
 465 from Ethiopian highlands due to lack of data (Haile et al., 2013) and coarse spatial resolution
 466 of the dataset (Huffman et al., 2007). However, Gebremicael et al. (2019) reported better
 467 performance of 3B43 for the Tekeze-Atibara basin, which is located in the northern
 468 mountainous area of Ethiopia.

469 Better correlation of SREs with observed rainfall was observed at monthly than at
 470 annual timescales for all products. This is consistent with studies that reported the performance
 471 of SREs improved with increased time aggregation that peaks at monthly timescale (Dembélé
 472 and Zwart, 2016; Katsanos et al., 2016; Zhao et al., 2017; Ayehu et al., 2018; Li et al., 2018;
 473 Guermazi et al., 2019). The weak agreement of SREs with observed data at annual timescale
 474 shows that the SREs considered in this study generally did not capture the interannual rainfall
 475 variability. In this regards, particularly the 3B43 product failed to capture annual rainfall
 476 variability compared to the other three SREs. Overall, all four SREs products overestimated

477 rainfall for the DRB by 10% for CHIRPS2 to 30% for IMERG6 and TAMSAT3 (Figure 5).
478 This finding is consistent with studies that reported overestimation of IMERG6 and 3B43
479 products for the alpine and gorge regions of China (Chen et al., 2019). However, Gebremicael
480 et al. (2019) reported underestimation of rainfall by CHIRPS2 for the Tekeze-Atbara basin,
481 which is a mountainous and arid basin in northern Ethiopia. Ayehu et al. (2018) also reported
482 slight underestimation of rainfall by CHIRPS2 for the upper Blue Nile Basin. The discrepancy
483 between our finding and the previous studies done for the basins in Ethiopia may be due to
484 differences in watershed characteristics such as topography, vegetation cover and climatic
485 conditions.

486 Generally, this study showed that the SREs products considered in this study exhibited
487 satisfactory rainfall detection and estimation capability for the DRB. The products could be
488 applicable for flood forecasting applications for the DRB (Toté et al., 2015). CHIRPS2
489 performed better than the other three SREs for annual, seasonal, and monthly timescales in
490 detecting and estimating rainfall for the basin. The superiority of CHIRPS2 was also reported
491 by previous studies for different parts of world (Katsanos et al., 2016; Dembélé and Zwart,
492 2016) including basins in Ethiopia (Bayissa et al., 2017; Ayehu et al., 2018; Dinku et al., 2018;
493 Gebremicael et al., 2019). For example, Dinku et al. (2018) reported better rainfall estimation
494 capability of CHIRPS2 for East Africa compared to African Rainfall Climatology version 2
495 (ARC2) and TAMSAT3 products. Ayehu et al. (2018) reported better performance of
496 CHIRPS2 for the Blue Nile Basin compared to ARC2 and TAMSAT3. Better performance of
497 CHIRPS2 has been attributed to the capability of the algorithm to integrate satellite, gauge and
498 reanalysis products and its high spatial and temporal resolution (Funk et al., 2015). On the
499 contrary, generally, the 3B43 rainfall product performed poorly for the DRB for all timescales.
500 This could be due to its coarse spatial resolution and lack of gauge-adjustment for highlands of
501 Ethiopia (Haile et al., 2013). The IMERG6 showed better rainfall detection and estimation
502 capability for the study area than the 3B43 product, which is consistent with findings of
503 previous studies (Huffman et al., 2015; Zhang et al., 2018; Zhang et al., 2019). Better
504 performance of IMERG6 is attributed to the inclusion of dual and high-frequency channels,
505 which improve light and solid precipitation detection capability (Huffman et al., 2015).

506 Hydrologic simulation performance evaluation result of SREs showed that accurate
507 characterization of rainfall variability is very critical for reliable hydrological predictions. This
508 finding is consistent with studies that reported that different precipitation datasets influence

509 model performance, parameter estimation and uncertainty in streamflow predictions (Sirisena
510 et al., 2018; Goshime et al., 2019). Overestimation of streamflow for all SREs products could
511 be resulted from uncertainty of SREs for extreme rainfall events at daily scale (Zhao et al.,
512 2017). The overestimated streamflow could also be attributed to overestimation of rainfalls by
513 the SREs as described in the previous sections and uncertainty of SWAT model.

514 Overall, this study showed that CHIRPS2 and IMERG6 predicted streamflow better
515 than the gauge rainfall and other two SREs products for the DRB. Superior hydrological
516 performance of SREs products compared to gauge rainfall data were also reported by many
517 other studies (Grusson et a., 2017; Bitew and Gebremichael, 2011; Goshime et al., 2019; Xian
518 et al., 2019; Li et al., 2018; Belete et al., 2020). For example, Bitew and Gebremichael (2011)
519 reported that satellite-based rainfall predicted streamflow better than gauge rainfall for complex
520 high-elevation basin in Ethiopia. Likewise, a bias-corrected CHIRP rainfall dataset resulted in
521 better streamflow prediction than a gauge rainfall dataset for Ziway watershed in Ethiopia
522 (Goshime et al., 2019).

523 The relatively poor performance of gauge rainfall compared to the CHIRPS2 and
524 IMERG6 shows that the existing rainfall gauges do not represent spatiotemporal variability of
525 rainfall in the DRB. The rain gauges are sparse, spatially uneven, and incomplete records for
526 the DRB. As previously mentioned, rain gauge density for the DRB is 0.32 per 1000 km²,
527 which is much lower than the World Meteorological Organization (WMO) recommendation of
528 one gauge per 100-250 km² for mountainous areas of tropical regions such as the DRB (WMO,
529 1994).

530 In contrast to several previous studies on SREs evaluation, the present study combined
531 statistical and hydrological performance evaluation in data scarce river basin of upper Blue
532 Nile basin, the Dhidhessa River Basin. This method is important to identify SREs that better
533 detect and estimate rainfall, and select application specific rainfall products such as for
534 hydrologic and climate change studies. The results of this study also highlights seasonal
535 dependence of rainfall detection and hydrologic performance capability of SREs for DRB and
536 similar basins in Ethiopia. In addition, the performance of IMERG6, which is the latest SREs
537 product, was evaluated for Ethiopian basin for the first time. Overall, this study showed that
538 CHIRPS2 and IMERG6 rainfall products performed best in terms of detecting and estimating
539 rainfall as well as predicting streamflow for the DRB.

540 **5. Conclusions**

541 Satellite rainfall estimate is an alternative rainfall data source for hydrological and
542 climate studies for data scarce regions like Ethiopia. However, SREs contain uncertainties
543 attributed to errors in measurement, sampling, retrieval algorithm and bias correction
544 processes. Moreover, the accuracy of rainfall estimation algorithm is influenced by topography
545 and climatic conditions of a given area. Therefore, SREs products should be evaluated locally
546 before they are used for any application. In this study, we examined the intrinsic data quality
547 and hydrological simulation performance of CHIRPS2, IMERG6, 3B42/3 and TAMSAT3
548 rainfall datasets for the DRB. The statistical evaluation results generally revealed that all four
549 SREs products showed promising rainfall estimation and detection capability for the DRB.
550 Particularly, all SREs captured the south-north declining rainfall patterns of the study area.
551 This could be due to the fact that all the SREs products were gauge adjusted and that they are
552 the latest and improved versions. However, all the SREs datasets overestimated rainfall for
553 DRB indicating that the rainfall products could be applicable for flood studies but not for
554 drought studies. The result also showed strong correlation of all SREs with measured rainfall
555 data for the monthly timescales than for the annual timescales, which shows that all the rainfall
556 products considered in this study cannot capture interannual rainfall variability.

557 The quantitative statistical indices showed that CHIRPS2 performed the best in
558 estimating and detecting rainfall events for the DRB at monthly as well as annual timescales.
559 This is likely due to the fact that CHIRPS2 was developed by merging satellite, reanalysis and
560 gauge datasets at high spatial resolution whereas 3B43 performed poorly for the basin.

561 The hydrological modelling based performance evaluation showed that ranges, best fit
562 values, and relative sensitivities of SWAT's calibration parameters varied with the rainfall
563 datasets. Overall, groundwater flow related parameters such as *GWQMN.gw*, *ALPHA_BF.gw*,
564 *GW_DELAY.gw* and *RCHRG_DP.gw* were found more sensitive for all rainfall products. This
565 showed that subsurface processes dominate hydrologic response of the DRB. The hydrological
566 simulation performance results also showed that all the rainfall products, including the
567 observed rainfall, overestimated streamflow especially the high flows. The peak streamflow
568 overestimation could be attributed to the uncertainty of SREs rainfall to predict at shorter
569 timescale (e.g., daily) and event rainfalls. The study showed CHIRPS2 and IMERG6 predicted
570 streamflow for the basin satisfactorily, and even outperformed performance of the gauge
571 rainfall. The relatively poor performance of the gauge rainfalls can be attributed to the fact that

572 the gauges are too sparse to accurately characterize rainfall variability in the basin. Overall,
573 CHIRPS2 and IMERG6 products seem to perform better for the DRB to detect rainfall events,
574 to estimate rainfall quantity, and to improve streamflow predictions. The new insights of this
575 study include: i) the SREs evaluation was done by combining statistical and hydrological
576 modelling methods; ii) the SREs considered in this study are the latest products reported best
577 in different studies, and IMERG6 is the most recent product evaluated in Ethiopian basin's for
578 the first time in this study and iii) the rainfall detection and estimation as well as streamflow
579 prediction capability of SREs is dependent on seasons. The results of this study are of interest
580 to both scientific communities and water resource managers, and this paper has made a good
581 contribution to improve understanding of the latest SREs for Ethiopia and the DRB. However,
582 streamflow simulation capability of the selected SREs products may be tested for other
583 hydrologic model to see if model types affect the results.

584 **Funding:** This research did not receive any specific grant from funding agencies in the public,
585 commercial, or not-for-profit sectors.

586 **Supplementary Materials:** Provided up on request.

587 **Author contributions**

588 Gizachew Kabite: Conceptualization, Data collection, analysis and interpretation, writing-
589 original draft preparation.

590 Misgana K. Muleta and Berhan Gessesse: Writing-review and editing. All authors have read
591 and agreed to the published version of the manuscript:

592 **Conflicts of Interest**

593 The authors declare no conflict of interest.

594 **Acknowledgments**

595 We are grateful to the Ethiopian Space Science and Technology Institute for providing partial
596 financial support for this research. We are also thankful to the developers of CHIRPS2,
597 IMERG6, TAMSAT3 and 3B42 datasets and for providing the data free of charge. The
598 National Meteorological Agency of Ethiopia and the Ethiopian Ministry of Water, Irrigation
599 and Energy are also acknowledged for providing climate and streamflow data, respectively.

600

601 **References**

- 602 Abbaspour, K.C.: SWAT-CUP 2012: SWAT Calibration and Uncertainty Programs-A
603 User Manual; Swiss Federal Institute of Aquatic Science and Technology: Eawag,
604 Switzerland. 2015.
- 605 Abbaspour, K.C., Yang, J., Maximov, I., Siber, R., Bogner, K., Mieleitner, J., Zobrist, J., and
606 Srinivasan, R.: Modelling hydrology and water quality in the pre-alpine/alpine
607 watershed using SWAT, *J. Hydrol.* 333, 413-430, 2007.
- 608 Abera, W., Brocca, L., and Rigon, R.: Comparative evaluation of different satellite
609 rainfall estimation products and bias correction in the Upper Blue Nile (UBN) basin,
610 *Atmos. Res.* 178-179,471-483, 2016.
- 611 Arnold, J.G., Moriasi,D.N., Gassman, P.W., K.C. Abbaspour, M.J. White, R.
612 Srinivasan, C. Santhi, R.D. Harmel, A. Van Griensven, M.W., and Liew, V.: SWAT:
613 Model use, calibration, and validation, *Trans. ASABE.* 55, 1491-1508, 2012.
- 614 Ayehu, G.T., Tadesse, T., Gessesse, B., and Dinku, T.: Validation of new satellite rainfall
615 products over the Upper Blue Nile Basin, Ethiopia, *Atmos. Meas. Tech.* 11, 1921-1936,
616 2018.
- 617 Bayissa, Y., Tadesse, T., Demisse, G., and Shiferaw, A.: Evaluation of satellite-based
618 rainfall estimates and application to monitor meteorological drought for the Upper Blue
619 Nile Basin, Ethiopia, *Remote Sens.* 9,669, 2017.
- 620 Behrangi, A., Khakbaz, B., Jaw,T. Ch., Kouchak, A. A., Hsu, K. and Sorooshian, S.:
621 Hydrologic evaluation of satellite precipitation products over a mid-size basin, *J.*
622 *Hydrolo.* 397,225-237, 2011.
- 623 Belete, M., Deng, J., Wang, K., Zhou, M., Zhu, E., Shifaw, E., and Bayissa, Y.: Evaluation
624 of satellite rainfall products for modeling water yield over the source region of Blue
625 Nile Basin, *Sci. Total Environ.* 708,134834, 2020.
- 626 Berne, A., and Krajewski, W.F.: Radar for hydrology: Unfulfilled promise or
627 unrecognized potential? *Adv. Water Resour.* 51, 357-366, 2013.
- 628 Bitew, M.M., and Gebremichael, M.: Evaluation of satellite rainfall products through
629 hydrologic simulation in a fully distributed hydrologic model, *Water Resour. Res.* 47,
630 1-11, 2011.

631 Brown, J.E.M.: An analysis of the performance of hybrid infrared and microwave satellite
632 precipitation algorithm over India and adjacent regions. *Remote Sens, Environ.* 101,
633 63-81, 2006.

634 Chen, J., Wang, Z., Wu, X., Chen, X., Lai, C., and Zeng, Z., Li, J.: Accuracy evaluation of
635 GPM multi-satellite precipitation products in the hydrological application over alpine
636 and gorge regions with sparse rain gauge network. *Hydrol. Res.* 50, 6, 2019.

637 Condom, T., Rau, P. and Espinoza, J. C.: Correction of TRMM 3B43 monthly
638 precipitation data over the mountainous areas of Peru during the period 1998-2007,
639 *Hydrol. Process.* 25, 1924-1933, 2011.

640 Conway, D.: The Climate and Hydrology of the Upper Blue Nile River, *The Geogr. J.* 1, 49-
641 62, 2000.

642 Dembélé, M., and Zwart, S, J.: Evaluation and comparison of satellite-based rainfall
643 products in Burkina Faso, West Africa, *Int. J. Remote Sens.* 37(17), 3995-4014, 2016.

644 de Goncalves, L.G.G., Shuttleworth, W.J., Nijssen, B., Burke, E.J., Marengo, J.A., Chou, S.C.,
645 Houser, P., and Toll, D.L.: Evaluation of model-derived and remotely sensed
646 precipitation products for continental South America, *J. Geoph. Res.*, 111: D16113,
647 2006.

648 Dinku, T., Chidzambwa, S., Ceccato, P., Connor, S. and Ropelewski, C.: Validation of
649 highresolution satellite rainfall products over complex terrain, *Int. J. Remote Sens.*,
650 29, 4097-4110, 2008.

651 Dinku, T., Funk, C., Peterson, P., Maidment, R., Tadesse, T., Gadain, H., and Ceccato., P.:
652 Validation of the CHIRPS satellite rainfall estimates over eastern Africa, *Quar. J.*
653 *Roy. Meteo. Soci.* 144, 292-312, 2018.

654 Dinku, T., Ruiz, F., Connor, S.J. and Ceccato, P.: Validation and Intercomparison of
655 Satellite Rainfall Estimates over Colombia, *J. Appl. Meteorol. Climatol.* 49, 1004-
656 1014, 2010.

657 Funk, C., Verdin, A., Michaelsen, J., Peterson, P., Pedreros, D. and Husak, G.: A global
658 satellite-assisted precipitation climatology, *Earth Syst. Sci., Data.* 7, 275-287, 2015.

659 Gassman, P.W., Sadeghi, A.M., and Srinivasan, R.: Applications of the SWAT model
660 special section: Overview and insights, *J. Environ. Qual.* 43, 1-8, 2014.

661 Gebremicael, T.G., Mohamed, Y.A., van der Zaag, P., Gebremedhin, M., Gebremeskel, G.,
662 Yazew, E., and Kifle, M.: Evaluation of multiple satellite rainfall products over the
663 rugged topography of the Tekeze-Atbara basin in Ethiopia, *Int. J. Remote Sen.*
664 40(11), 4326-4345, 2019.

665 Gebremichael, M., Bitew, M.M., Hirpa, F.A., and Tesfay, G. N.: Accuracy of satellite
666 rainfall estimates in the Blue Nile Basin: Lowland plain versus highland mountain,
667 *Water Resour. Res.* 50, 8775-8790, 2014.

668 Geological Survey of Ethiopia (GSE): Geology of the Nekemte and Gimbi Area. Sheet
669 Number: NC-37-9 and NC-36-12, respectively. Unpublished, 2000.

670 Goshime, D.W., Absi, R., and Ledésert, B.: Evaluation and Bias Correction of CHIRP
671 Rainfall Estimate for Rainfall-Runoff Simulation over Lake Ziway Watershed,
672 Ethiopia, *Hydrology*, 6:68, 2019.

673 Grusson, Y., Antil, F., Sauvage, S., and Perz, S.: Testing the SWAT Model with Gridded
674 Weather Data of Different Spatial Resolution. *Water*, 9:54, 2017.

675 Guerhazi, E., Milano, M., and Reynard, E.: Performance evaluation of satellite-based
676 rainfall products on hydrological modelling for a transboundary catchment in northwest
677 Africa, *Theo. App. Clim.* 138, 1695-1713, 2019.

678 Habib, E., Haile, A. T., Tian, T., and Joyce, R. J.: Evaluation of the High-Resolution
679 CMORPH Satellite Rainfall Product Using Dense Rain Gauge Observations and Radar-
680 Based Estimates, *J. Hydrmeteo.*, 13 (6), 1784-1798, 2012.

681 Haile, A. T., Habib, E., Elsaadani, M., and Rientjes, T.: Intercomparison of satellite
682 rainfall products for representing rainfall diurnal cycle over the Nile basin, *Int. J. Appl.*
683 *Earth Obs.* 21, 230-240, 2013.

684 Hu, Q., Yang, D., Li, Z., Mishra, A.K., Wang, Y., and Yang, H.: Multi-scale evaluation of
685 six high-resolution satellite monthly rainfall estimates over a humid region in China
686 with dense rain gauges, *Int. J. Remote Sens.* 35, 1272-1294, 2014.

687 Huffman, G. J., Bolvin, D. T., Nelkin, E. J., Wolff, D. B., Adler, R. F., Gu, G., Hong, Y.,
688 Bowman, K. P., and Stocker, E. F.: The TRMM Multisatellite Precipitation
689 Analysis (TMPA): quasiglobal, multiyear, combined-sensor precipitation estimates at
690 fine scales, *J. Hydrometeorol.* 8, 38-55, 2007.

691 Huffman, G.J., Bolvin, D.T., Braithwaite, D., Hsu, K., Joyce, R.J., Kidd, C., Nelkin, E.J., and
692 Xie, P.: Algorithm Theoretical Basis Document (ATBD), 2015.

693 Huffman, G.J., Bolvin, D.T., Braithwaite, D., Hsu, K., Joyce, R., Xie, P., and Yoo, S.H.:
694 NASA global precipitation measurement (GPM) integrated multi-satellite retrievals
695 for GPM (IMERG). In Algorithm Theoretical Basis Document (ATBD); NASA/GSFC:
696 Greenbelt, MD, USA, 2014.

697 Jiang, S., Liu, S., Ren, L., Yong, B., Zhang, L., Wang, M., Lu, Y., and He, Y.: Hydrologic
698 Evaluation of Six High Resolution Satellite Precipitation Products in Capturing
699 Extreme Precipitation and Streamflow over a Medium-Sized Basin in China, *Water*,
700 10, 25, 2017.

701 Joyce, R. J., Janowiak, J. E., Arkin, P. A., and Xie, P.: CMORPH: a method that produces
702 global precipitation estimates from passive microwave and infrared data at high spatial
703 and temporal resolution, *J. Hydrometeo.* 5, 487-503, 2004.

704 Kabite, G., and Gessesse, G.: Hydro-geomorphological characterization of Dhidhessa
705 River Basin, Ethiopia, *Int. Soil and Water Cons. Res.* 6, 175-183, 2018.

706 Kabite, G., Muleta, M.K., and Gessesse, B.: Spatiotemporal land cover dynamics and
707 drivers for Dhidhessa River Basin (DRB), Ethiopia, *Mod. Earth Sys. Environ.* 6,
708 1089-1103, 2020.

709 Katsanos, D., Retalis, A., and Michaelides. S.: Validation of a high-resolution
710 precipitation database (CHIRPS) over Cyprus for a 30-year period, *Atmos.*
711 *Res.* 169, 459-464, 2016.

712 Kidd, C., and Huffman, G.: Global precipitation measurement. *Meteorol. Appl.* 18,334-
713 353, 2011.

714 Kidd, C., Bauer, P., Turk, J., Huffman, G.J., Joyce, R., Hsu, K.L., and Braithwaite, D.:
715 Intercomparison of high-resolution precipitation products over northwest Europe. *J.*
716 *Hydrometeorol.* 13, 67-83, 2012.

717 Kimani, M.W., Hoedjes, J.C.B., and Su, Z.: An assessment of satellite-derived rainfall
718 products relative to ground observations over East Africa, *Remote Sens.* 9(5), 430,
719 2017.

720 Lakew, H.B., Moges, S.A., and Asfaw, D.H.: Hydrological Evaluation of Satellite and
721 Reanalysis precipitation products in the Upper Blue Nile Basin: A case study of Gilgal
722 Abbay, *Hydrology*, 4, 39, 2017.

723 Lemann, T., Roth, V., Zeleke, G., Subhatu, A., Kassawmar, T., and Hurni, H.: Spatial and
724 Temporal Variability in Hydrological Responses of the Upper Blue Nile basin,
725 Ethiopia, *Water*, 11, 21, 2019.

726 Li, D., Christakos, G., Ding, X., and Wu, J.: Adequacy of TRMM satellite rainfall data in
727 driving the SWAT modeling of Tiaoxi catchment (Taihu lake basin, China), *J. Hydr.*
728 556, 1139-1152, 2018.

729 Maggioni, V., Meyers, P.C., and Robinson, M.D.: A Review of Merged High-Resolution
730 Satellite Precipitation Product Accuracy during the Tropical Rainfall Measuring
731 Mission (TRMM) Era, *J. Hydrometeor.* 17, 1101-1117, 2016.

732 Maidment, R., Emily, B., and Matt, Y.: TAMSAT Daily Rainfall Estimates (Version 3.0).
733 University of Reading. Dataset. doi.org/10.17864/1947.112, 2017.

734 Meng, J., Li, Z., Hao, J., Wang, S. Q.: Suitability of TRMM Satellite Rainfall in Driving
735 Distributed Hydrological Model in the Source Region of Yellow River. *J. Hydrol.*
736 509, 320-332, 2014.

737 Moriasi, D. N., Arnold, J. G., Van Liew, M. W., Bingner, R.L., Harmel, R.D., and Veith, T.L.:
738 Model evaluation guidelines for systematic quantification of accuracy in watershed
739 simulations. *Trans. American Socie. Agr. Bio. Eng.* 50(3), 885-900, 2007.

740 Nebuloni, R., D'Amico, M., Cazzaniga, G., De Michele, C., and Deidda, C.: Rainfall
741 estimate using Commercial Microwave Links (CML): first outcomes of the
742 MOPRAM project. EGU2020-1040, 19th EGU General Assembly, EGU2017,
743 proceedings from the conference held 23-28 April, 2017 in Vienna, Austria., p.18576.
744 <https://doi.org/10.5194/egusphere-egu2020-1040>, 2020.

745 Neitsch, S.L., Arnold, J.G., Kiniry, J.R., and Williams, J.R.: Soil & Water Assessment
746 Tool-Theoretical Documentation Version 2009. Texas Water Resour. Inst, 2009.

747 Nesbitt, S.W., Gochis, D.J., and Lang, T.J.: The diurnal cycle of clouds and precipitation
748 along the Sierra Madre Occidental observed during NAME-2004: Implications for
749 warm season precipitation estimation in complex terrain, *J. Hydrometeoro.* 9, 728-
750 743, 2008.

751 Nguyen, T.H., Masih, I., Mohamed, Y.A., and Van Der Zaag, P.: Validating rainfall-
752 runoff modelling using satellite-based and reanalysis precipitation products in the Sre
753 Pok catchment, the Mekong River basin, *Geosciences*, 8(5), 164-184, 2018.

754 Oromia Water Works Design and Supervision Enterprise (OWWDSE): Dhidhessa Sub-
755 Basin Soil Survey Report. Dhidhessa-Dabus Integrated Land Use Planning Study
756 Project. Unpublished, 2014.

757 Roth, V., Lemann, T., Zeleke, G., Subhatu, A.T., Nigussie, T.K., and Hurni, H.: Effects of
758 climate change on water resources in the upper Blue Nile Basin of Ethiopia, *Heliyon*,
759 4(2018) e00771, 2018.

760 Sahlaoui, Z., and Mordane, S.: Radar Rainfall Estimation in Morocco: Quality
761 Control and Gauge Adjustment. *Hydrology*, 6 (2):41, 2019.

762 Smiatek, G., Keis, F., Chwala, C., Fersch, B., and Kunstmann, H.: Potential of
763 commercial microwave link network derived rainfall for river runoff simulations.
764 *Environmental Research Letter*, 12, 034026, 2017.

765 Seyyedi, H., Angagnostou, E.N., Beinghley, E., and McCollum, J.: Hydrologic evaluation
766 of satellite and reanalysis precipitation datasets over a mid-latitude basin, *Atm.*
767 *Res.* 164-165, 37-48, 2015.

768 Sirisena, T.A.J.G., Maskey, S., Ranasinghe, R., and Babel, M.S.: Effects of different
769 precipitation inputs on streamflow simulation in the Irrawaddy River Basin, Myanmar.
770 *J. Hyd.: Reg. Studies.* 19, 265-278, 2018.

771 Sorooshian, S., Hsu, K.-L., Gao, X., Gupta, H. V., Imam, B., and Braithwaite, D.: Evaluation
772 of PERSIANN system satellite-based estimates of tropical rainfall, *B. Am. Meteorol.*
773 *Soc.* 81, 2035-2046, 2000.

774 Stisen, S., and Sandholt, I.: Evaluation of remote-sensing-based rainfall products through
775 predictive capability in hydrological runoff modeling, *Hydrol. Proce.* 24, 879-
776 891, 2010.

777 Su, J., Lü, H., Wang, J., Sadeghi, A., and Zhu, Y.: Evaluating the Applicability of Four
778 Latest Satellite-Gauge Combined Precipitation Estimates for Extreme Precipitation
779 and Streamflow Predictions over the Upper Yellow River Basins in China. *Remote*
780 *Sens.* 9, 1176, 2017.

781 Tapiador, F.J., Turk, F.J., Petersen, W., Hou, A.Y., García-Ortega, E., Machado, L.A.T.,
782 Angelis, C.F., Salio, P., Kidd, C., Huffman, G.J., et al., Global precipitation
783 measurement: Methods, datasets and applications. *Atmos. Res.* 104-105, 70-97, 2012.

784 Thiemi, V., Rojas, R., Zambrano-Bigiarini, M., and Roo, A. D.: Hydrological evaluation
785 of satellite-based rainfall estimates over the Vota and Baro-Akobo Basin, *J.*
786 *Hydrology.* 499, 324-333, 2013.

787 Tong, K., Su, F., Yang, D., and Hao, Z.: Evaluation of satellite precipitation retrievals and
788 their potential utilities in hydrologic modeling over the Tibetan Plateau, *J. Hydrol.*
789 519, 423-437, 2014.

790 Toté, C., D. Patricio, H. Boogaard, R. Van der Wijngaart, E. Tarnavsky, and Funk, C.:
791 Evaluation of Satellite Rainfall Estimates for Drought and Flood Monitoring in
792 Mozambique, *Remote Sens.* 7 (2), 1758-1776, 2015.

793 Vernimmen, R.R., Hooijer, A., Aldrian, E., and Van Dijk, A.I.: Evaluation and bias
794 correction of satellite rainfall data for drought monitoring in Indonesia, *Hydrol.*
795 *Earth Syst. Sci.*, 16, 133-146, 2012.

796 Villarini, G., Krajewski, W.F.: Review of the different sources of uncertainty in single
797 polarization radar-based estimates of rainfall. *Surv. Geophys.*, 31, 107-129, 2010.

798 WMO: World Meteorological Organization Guide to Hydrological Practices: Data
799 Acquisition and Processing, Analysis, Forecasting and Other Applications. Geneva:
800 Switzerland, 1994.

801 Worqlul, A.W., Maathuis, B., Adem, A.A., Demissie, S.S., Langan, S., and Steenhuis, T.S.:
802 Comparison of rainfall estimations by TRMM3B42, MPEG and CFSR with
803 ground-observed data for the Lake Tana basin in Ethiopia, *Hydrol. Earth Syst. Sci.*
804 18, 4871-4881, 2014.

805 Wu, H., and Chen, B.: Evaluating uncertainty estimates in distributed hydrological
806 modeling for the Wenjing River watershed in China by GLUE, SUFI-2, and ParaSol
807 methods, *Ecol. Eng.* 76,110-121, 2015.

808 Xian, L., Wenqi, W., Daming, H., Yungang, L., and Xuan., J.: Hydrological Simulation
809 Using TRMM and CHIRPS Precipitation Estimates in the Lower Lancang-Mekong
810 River Basin. *China Geog. Sci.* 29(1), 13-25, 2019.

811 Xie, P., and Arkin, A.: An Inter-comparison of Gauge Observations and Satellite Estimates
812 of Monthly Precipitation, *J. Appl. Meteorol.* 34, 1143-1160, 1995.

813 Xue, X., Hong, Y., Limaye, A.S., Gourley, J.J., Huffman, G.J., Khan, S.I., and Chen, S.:
814 Statistical and Hydrological Evaluation of TRMM-Based Multi-Satellite Precipitation
815 Analysis over the Wangchu Basin of Bhutan: Are the Latest Satellite Precipitation
816 Products 3B42V7 Ready for Use in Ungauged Basins? *J. Hydrol.* 499, 91-99, 2013.

817 Yohannes, O.: Water Resources and Inter-Riparian Relations in the Nile Basin: The
818 Search for an integrative Discourse. 270, 2008.

819 Yong, B., Chen, B., Gourley, J.J., Ren, L., Hong, Y., Chen, X., Wang, W., Chen, S., and Gong,
820 L.: Inter-comparison of the Version-6 and Version-7 TMPA precipitation products
821 over high and low latitudes basins with independent gauge networks: is the
822 newer version better in both real-time and post-real-time analysis for water resources
823 and hydrologic ext, *J. Hydrol.* 508, 77-87, 2014.

824 Zeweldi, D.A., Gebremichael, M., and Downer, C.W.: On CMORPH rainfall for streamflow
825 simulation in a small, Hortonian watershed. *J. Hydrometeorol.* 12, 456-466, 2011.

826 Zhang, C., Chen, X., Shao, H., Chen, S., Liu, T., Chen, C., Ding, Q., and Du, H.: Evaluation
827 and Inter-comparison of High-Resolution Satellite Precipitation Estimates-GPM,
828 TRMM, and CMORPH in the Tianshan Mountain Area. *Remote sens.* 10, 1543, 2018.

829 Zhang, Z., Tian, J., Huang, Y., Chen, X., Chen, S., and Duan, Z.: Hydrologic Evaluation of
830 TRMM and GPM IMERG Satellite-Based Precipitation in a Humid Basin of China.
831 Remote Sens. 11, 431, 2019.

832 Zhao, Y., Xie, Q., Lu, Y., and Hu, B.: Hydrologic Evaluation of TRMM Multisatellite
833 Precipitation Analysis for Nanliu River Basin in Humid Southwestern China. Scie.
834 Reports, 7, 2470, 2017.

835 Zhou, J., Liu, Y., Guo, H., and He, D.: Combining the SWAT model with sequential
836 uncertainty fitting algorithm for streamflow prediction and uncertainty analysis for the
837 Lake Dianchi Basin, China. Hydrol. Process. 28, 521-533, 2014.

838

839 **Appendix**

840 Appendix Table 1. List of rain gauge stations used for SREs evaluation.

S. No	Stations	Latitude	Longitude	Elevation	Remark
1	Bedele	8.3	36.2	2011	Within the basin
2	Gatira	8.0	36.2	2358	Within the basin
3	Gimbi	9.2	35.8	1970	Within the basin
4	Nedjo	9.5	35.5	1800	Within the basin
5	Anger	9.3	36.3	1350	Within the basin
6	Gida Ayana	9.9	36.9	1850	Within the basin
7	Arjo	8.5	36.3	2565	Within the basin
8	Jimma*	7.8	36.4	1718	Within the basin
9	Nekemte*	9.1	36.5	2080	Within the basin
10	Shambu	9.6	37.1	2460	Near the basin
11	SibuSire	9.0	35.9	1826	Within the basin
12	Bure	8.2	35.1	1750	Near the basin
13	Sokoru	7.9	37.4	1928	Near the basin
14	Gore	8.1	35.5	2033	Near the basin

841 *systematically removed from using for calibration as they are already used for SREs calibration.